Open and Closed Edges of Graphene Layers

Zheng Liu,[1,*] Kazu Suenaga,[1,*] Peter J. F. Harris,[2] and Sumio Iijima[1]

[1]*Nanotube Research Center, National Institute of Advanced Industrial Science and Technology (AIST), Tsukuba 305-8565 Japan*

[2]*Centre for Advanced Microscopy, J.J. Thomson Physical Laboratory, University of Reading, Whiteknights, Reading RG6 6AF, United Kingdom*

(Received 9 September 2008; published 5 January 2009)

Edge structures of thermally treated graphite have been studied by means of atomically resolved high-resolution TEM. The method for the determination of a monolayer or more than one layer graphene sheets is established. A series of tilting experiments proves that the zigzag and armchair edges are mostly closed between adjacent graphene layers, and the number of dangling bonds is therefore minimized. Surprisingly bilayer graphene often exhibits *AA* stacking and is very hard to distinguish from a single graphene layer. Open edge structures with carbon dangling bonds can be found only in a local area where the closed (folding) edge is partially broken.

DOI: 10.1103/PhysRevLett.102.015501 PACS numbers: 81.05.Uw, 61.46.−w, 68.37.Og

Graphene, a single layer sheet of graphite, is the basic structural element of all other graphitic materials such as graphite, carbon nanotubes, and fullerenes. The potential applications in condensed matter physics and electronics have boosted interest in graphene especially in the structure and properties of its edges [1]. The presence of open edges in graphene should produce essential differences in electronic features compared to other sp^2 based nanocarbon π electron systems such as ball-shaped fullerenes without edges or cylinder-shaped carbon nanotubes with a negligible contribution of edges. Recent studies indeed clarified the unconventional electronic features of graphene not only the monolayer but also the bilayer graphene sheet [2–12]. According to theoretical predictions, zigzag edges give an extra nonbonding π electron state to the graphene sheet which means the energy of the graphene sheet with zigzag edges is not stable compared with that of the graphene sheet with armchair edges [13]. It was also theoretically suggested that because of the localized spins around zigzag edge, which give a strong exchange interaction, the appearance of ferromagnetism depends on the structures of graphene edges. In order to corroborate the unusual electronic features of graphene, investigation of the edge structures at an atomic scale is extremely important. Several studies have been reported using scanning tunneling microscopy (STM) to investigate the well defined graphene edges terminated by hydrogen in ultrahigh vacuum conditions [14,15]. Folding of monolayer and bilayer graphene, i.e., closed edges, were also studied by several groups by using the transmission electron microscope (TEM) [16,17]; however, no confirming evidence for the presence of open edges has been so far provided. Neither has the actual edge structure of graphene ever been atomically revealed.

In this study, we report direct imaging of the edges of thermally treated graphite and show the evidence for a coexistence of closed and open edges in graphene (schematized in Fig. 1). A high-resolution transmission electron microscope (HR-TEM) was operated at 120 kV with a point resolution better than 0.106 nm. Bilayer graphene with *AA* stacking has been carefully distinguished from a monolayer graphene by means of a series of tilting experiments.

Commercially available pyrolytic graphite powders (Ito Kokuen Co., Ltd.) were heated to 2000 °C for 3 hours in a vacuum ($<1 \times 10^{-2}$ Pa) after being ground by a pestle in a mortar. This heat treatment made the edge of graphene sheets (a single layer or a few layers sheet) to be neat. After heat treatment the graphite powders were ground again and then dispersed in ethanol (99.9 vol. %) by ultrasonication and the suspension was dropped onto a carbon microgrid for HR-TEM observation. A field emission TEM JEM-2010F (JEOL) equipped with a CEOS post specimen spherical aberration corrector (C_s corrector) was operated at 120 kV for the HR-TEM imaging with high resolution and high contrast so that the electron-beam damage of the specimen is reduced as much as possible (the beam density during the observations is less than 62 800 electrons/(nm^2 · sec) or 1.0 C/(cm^2 · sec). Thus the electron-beam induced defects such as the atomic vacancies and the dislocation cores found in [18] were not observed in this study. The specimen was kept at the ambient temperature during the observation. The C_s was set to less than 1 μm and the HR-TEM images were recorded at the slightly underfocused condition. A Gatan 894 CCD camera was used for digital recording of the HR-TEM images. A sequence of HR-TEM images (20 to

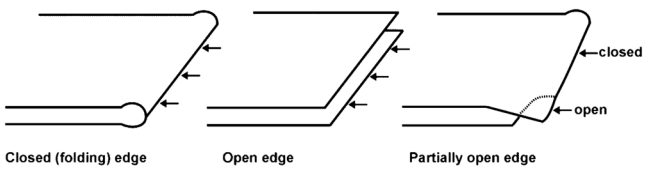

FIG. 1. Schematic presentations for closed, open, and partially open edge of a bilayer graphene.

40 frames) was recorded, with a 1 s exposure time for each. After drift compensation, some frames can be superimposed to increase the signal-to-noise (SN) ratio for display. Electron energy loss spectroscopy (EELS) was performed on the same specimen with a focused electron beam (several nm in diameter) by using the post column spectrometer (Gatan Enfina). Image simulations were carried out by using MACTEMPAS software package.

In this experiment, commercial graphite samples were studied before and after heat treatment. Although both samples show a layered structure, the specimen after 2000 °C heat treatment indeed shows the well developed facet on the verges of graphite. The wavy edges of graphite before heat treatment [Fig. 2(a)] transform to straight-lines after the heat treatment [Fig. 2(b)]. It seems that the heat treatment reduced amount of defects near all the verges of graphite. The faceted edge lines mostly run through in the zigzag and armchair directions (see the arrow-heads) with an intersecting angle of 30° degree and often appear in groups of two (or more). An edge line corresponds to a closed (folding) edge of bilayer graphene, and the paired edge lines correspond to the two parallel closed edges of four graphene sheets as illustrated in the Fig. 2(c) [see also our figure files (fig. S1) in the supplementary material [19]].

A typical HR-TEM image of a single edge line region is shown in Fig. 3(a). The incident beam direction was along the *c* axis of the graphene layers. The zigzag and armchair directions are marked, respectively, with white and black arrowheads. Note that this is the edge of "bilayer graphene" with the *AA* stacking in which the edges are closed (folded) as illustrated in Fig. 3(c). The number of the graphene layers can be known from the number of the edge line in the HR-TEM image; however, great attention should be paid to discriminate the number of the graphene layers, otherwise a bilayer graphene is easily confused with a single graphene layer. The difficulty in determining the stacking sequence has already been shown by the Raman spectroscopy studies [20,21] in which the spectroscopy of bilayer graphene sheets with arbitrarily misorientation was similar with that of a single layer. Here a series of tilting experiments under the HR-TEM observation has been employed to discriminate a bilayer graphene from the monolayer graphene. When the graphene sheet is just in the [001] direction, the hexagonal contrast of six *C* atoms will appear in the HR-TEM images for both the monolayer and bilayer graphene sheet. If the graphene is tilted deviating from the [001] direction for 20°, the hexagonal contrast will still remain in the HR-TEM images for monolayer graphene but the linear contrast will appear instead of the

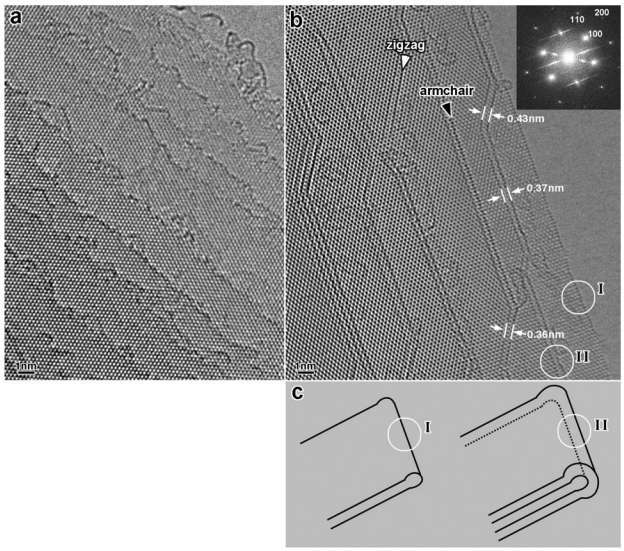

FIG. 2. (a) HR-TEM image of the graphite powders before heat treatment shows wavy edge structures, (b) HR-TEM image of the pyrolytic graphite powders after heat treatment shows the straight edge lines. Each edge line corresponds to a closed edge of bilayer graphene (c). The inserted Fourier transform diffractogram of the HR-TEM image indicates the 0.106 nm [(200) spots] resolution was achieved.

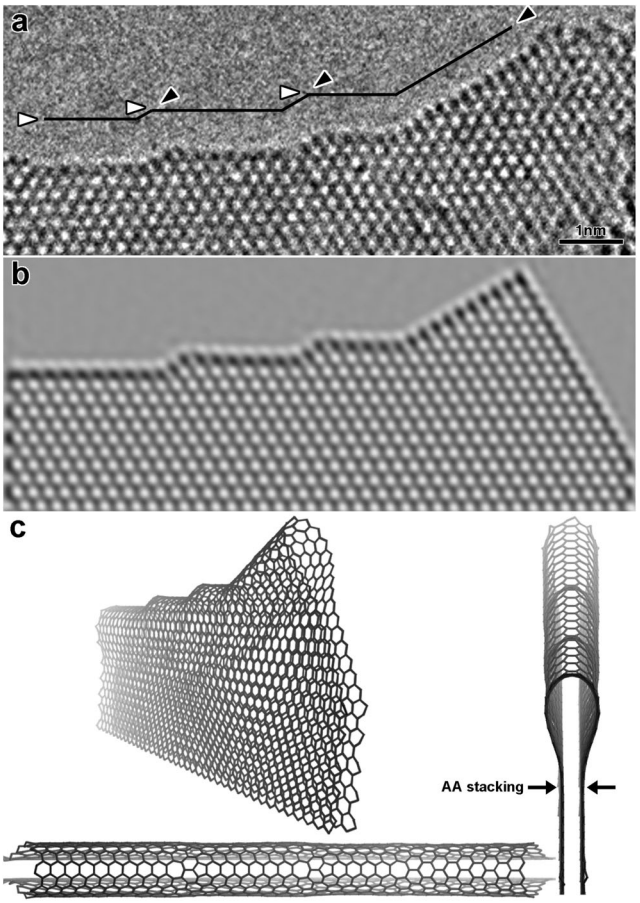

FIG. 3. (a) HR-TEM image showing the closed bilayer graphene. The zigzag and armchair directions are marked with white and black arrowheads. A simulated image (b) using a model with the *AA* stacking of the folded monolayer graphene (c). Each intersecting point between the armchair and the zigzag areas needs a pentagon-heptagon pair.

hexagonal contrast in the HR-TEM images for the bilayer graphene sheet [for the details see our figure files (fig. S2) provided in the supplementary material [19]]. The closed edge can be well explained by a folding model which was made by adding a half (10,0) carbon nanotube and a half (6,6) carbon nanotube to connect the edges of adjacent layers for the armchair and zigzag edge lines, respectively. A pentagon-heptagon pair is required for each intersecting point and then the whole model has been geometrically optimized by using the molecular mechanics with the $MM+$ force field method [Fig. 3(c)]. A HR-TEM simulation [Fig. 3(b)] based on this constructed model shows a perfect fit with the experiment and therefore the closed (folded) edge in a bilayer graphene with the *AA* stacking is confirmed.

We have confirmed with hundreds of TEM micrographs that most of the edges in the thermally treated graphite are completely closed and appear in a pair (or more) of straight lines in the HR-TEM images. The closed edge is quite reasonable because it can minimize the number of carbon dangling bonds. The total length of the armchair and zigzag edge lines are found to be in the ratio of 55 to 45, which may not directly reflect a theoretical prediction in which the armchair edge is more favorable than the zigzag edge since the calculation was performed on the open edges [13]. No theoretical consideration about the energetics of closed edges can be found in literature.

Another important implication of the above experiment is, surprisingly, the presence of bilayer graphene with *AA* stacking in a high probability. As widely known, the most common Bernal graphite has *AB* stacking along the *c* axis [22]. Simple hexagonal graphite with the *AA* stacking sequence [23,24] and rhombohedral graphite with the *ABC* stacking sequence [25,26] have also been repeatedly reported. Here in our experiments, the *AA* stacking seems to be dominant at least for some regions with the reduced number of layers (See also the edge-on HR-TEM images in figure files (fig. S1) in the supplementary material [19]). Because the electronic excitations and the magnetoelectronic properties of graphite should strongly depend on the interlayer interactions and the stacking sequences [27,28], the *AA* stacking bilayer graphene should be also an intriguing material.

No monolayer graphene has been found in our experiments. Therefore the presence of the open edge cannot be confirmed in a wide region. However, we have identified at least small regions of open edges in the thermally treated graphite specimens, where the closed edges are partially broken (as illustrated in Fig. 1). The heat treatment does reduce most of the defects near the verges of graphite so that such open edges were seldom found. Figure 4(a) shows a local region of the open edge along the lines of the closed armchair edge region. An isolated hexagon of carbon atoms extruding from the armchair edge can be clearly seen where the closed edge is partially broken

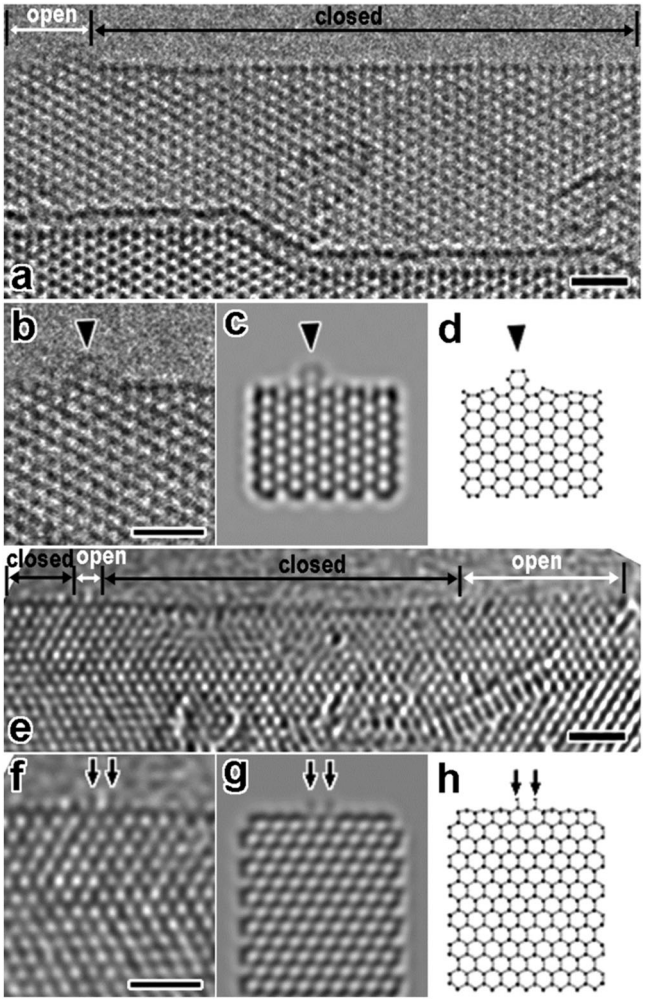

FIG. 4. HR-TEM image of partially open edges for armchair (a–d) and zigzag edges (e)–(h). (B) An isolated hexagon extruding from the armchair edge where the closed edge is partially broken (a), (c) A simulated image based on a model described in (d). (e) An open edge structure of the zigzag edge. Two carbon atoms are debonded and protruded from the closed edge (f). (g) A simulated image based on the Klein model (h). The scale bar = 1 nm.

[enlarged in Fig. 4(b)]. Figure 4(c) is a simulated image using a model involving a possible vibration of the protruding four carbon atoms with a slight beam tilt during the observation [Fig. 4(d)]. The simulated image with a blurred contrast gives a good match with the experimental HR-TEM image. This is the first proof for the presence of an open edge with the bare carbon atoms.

A similar situation of carbon atoms with dangling bonds can be also found in the zigzag edge [Figs. 4(e)–4(g)]. In a part of the closed zigzag edge, some dark contrast extruding from the closed edge can be occasionally found [Fig. 4(e)]. This contrast can be attributed to the carbon atoms with dangling bonds resulting from the broken closed edge. An open edge model involving the vibration of the carbon atoms which is employed to explain the

blurred contrast is shown in Fig. 4(h). A HR-TEM simulation based on the model fits very well with the experimental HR-TEM image. The open edge structure is known as the Klein edge [29,30] and has been long predicted by theory but experimentally proved here for the first time. Such an open edge can be generated only at the closed edge (folding areas) but not in the flat graphene part, suggesting that the folding part (with a high curvature) was more energetically unstable.

It is indeed reasonable that the graphene edges are more likely to be closed because of the reduced number of dangling bonds. An open edge may be easily terminated by -OH or -COOH in ambient conditions, and our EELS local analysis does show the trace of oxygen near the edge region [see the EELS spectrum in figure files (fig. S3) provided through the in the supplementary material [19]]. The *AA* stacking structure found in this study may be triggered by the formation of closed edge in order to reduce the local strains during the heat treatment.

This work is partially supported by CREST and Grant-in-Aid from MEXT (19054017).

*To whom correspondence should be addressed.
liu-z@aist.go.jp
suenaga-kazu@aist.go.jp

[1] T. Enoki, Y. Kobayashi, and K. Fukui, Int. Rev. Phys. Chem. **26**, 609 (2007).
[2] K. S. Novoselov, A. K. Geim, S. V. Morozov, D. Jiang, Y. Zhang, S. V. Dubonos, I. V. Grigorieva, and A. A. Firsov, Science **306**, 666 (2004).
[3] K. S. Novoselov, A. K. Geim, S. V. Morozov, D. Jiang, M. I. Katsnelson, I. V. Grigorieva, S. V. Dubonos, and A. A. Firsov, Nature (London) **438**, 197 (2005).
[4] C. L. Kane and E. J. Mele, Phys. Rev. Lett. **95**, 226801 (2005).
[5] T. Ohta, A. Bostwich, T. Seyller, K. Horn, and E. Rotenberg, Science **313**, 951 (2006).
[6] K. S. Novoselov, Z. Jiang, Y. Zhang, S. V. Morozov, H. L. Stormer, U. Zeitler, J. C. Maan, G. S. Boebinger, P. Kim, and A. K. Geim, Science **315**, 1379 (2007).
[7] J. C. Meyer, A. K. Geim, M. I. Katsnelson, K. S. Novoselov, T. J. Booth, and S. Roth, Nature (London) **446**, 60 (2007).
[8] E. V. Castro, K. S. Novoselov, S. V. Morozov, N. M. R. Peres, J. M. B. Lopes dos Santos, and J. Nilsson, Phys. Rev. Lett. **99**, 216802 (2007).
[9] R. Dillenschneider and J. H. Han, Phys. Rev. B **78**, 045401 (2008).
[10] B. Sahu, H. Min, A. H. MacDonald, and S. K. Banerjee, Phys. Rev. B **78**, 045404 (2008).
[11] E. V. Castro, N. M. R. Peres, J. M. B. Lopes dos Santos, A. H. Castro Neto, and F. Guinea, Phys. Rev. Lett. **100**, 026802 (2008).
[12] Y. Barlas, R. Côté, K. Nomura, and A. H. MacDonald, Phys. Rev. Lett. **101**, 097601 (2008).
[13] S. E. Stein and R. L. Brown, J. Am. Chem. Soc. **109**, 3721 (1987).
[14] J. C. Meyer, A. K. Geim, M. I. Katsnelson, K. S. Novoselov, D. Obergfell, S. Roth, C. Girit, and A. Zettl, Solid State Commun. **143**, 101 (2007).
[15] A. C. Ferrari, J. C. Meyer, V. Scardaci, C. Casiraghi, M. Lazzeri, F. Mauri, S. Piscanec, D. Jiang, K. S. Novoselov, S. Roth, and A. K. Geim, Phys. Rev. Lett. **97**, 187401 (2006).
[16] Y. Kobayashi, K. Fukui, T. Enoki, K. Kusakabe, and Y. Kaburagi, Phys. Rev. B **71**, 193406 (2005).
[17] Y. Kobayashi, K. Fukui, T. Enoki, and K. Kusakabe, Phys. Rev. B **73**, 125415 (2006).
[18] M. H. Gass, U. Bangert, A. L. Bleloch, P. Wang, R. R. Nair, and A. K. Geim, Nature Nanotech. **3**, 676 (2008).
[19] See EPAPS Document No. E-PRLTAO-102-052901 for supplementary figures. For more information on EPAPS, see http://www.aip.org/pubservs/epaps.html.
[20] Z. H. Ni, Y. Y. Wang, T. Yu, Y. M. You, and Z. X. Shen, Phys. Rev. B **77**, 235403 (2008).
[21] P. Poncharal, A. Ayari, T. Michel, and J.-L. Sauvajol, Phys. Rev. B **78**, 113407 (2008).
[22] J. C. Charlier, J. P. Michenaud, and X. Gonze, Phys. Rev. B **46**, 4531 (1992).
[23] J. C. Charlier, J. P. Michenaud, X. Gonze, and J. P. Vigneron, Phys. Rev. B **44**, 13 237 (1991).
[24] H.-V. Roy, C. Kallinger, and K. Sattler, Surf. Sci. **407**, 1 (1998).
[25] J. C. Charlier, X. Gonze, and J. P. Michenaud, Carbon **32**, 289 (1994).
[26] M. Aoki and H. Amawasi, Solid State Commun. **142**, 123 (2007).
[27] C. L. Lu, C. P. Chang, and M. F. Lin, Eur. Phys. J. B **60**, 161 (2007).
[28] J. H. Ho, C. L. Lu, C. C. Hwang, C. P. Chang, and M. F. Lin, Phys. Rev. B **74**, 085406 (2006).
[29] D. J. Klein, Chem. Phys. Lett. **217**, 261 (1994).
[30] K. Kusakabe and M. Maruyama, Phys. Rev. B **67**, 092406 (2003).